UCRL-JC-130437
PREPRINT

Shipping Container Response to Three Severe Railway Accident Scenarios

G. C. Mok
L. E. Fischer
S. S. Murty
M. C. Witte

This paper was prepared for submittal to the
1998 American Society of Mechanical Engineers Joint Pressure Vessels and Piping Conference
San Diego, CA
July 26-31, 1998

April 1998

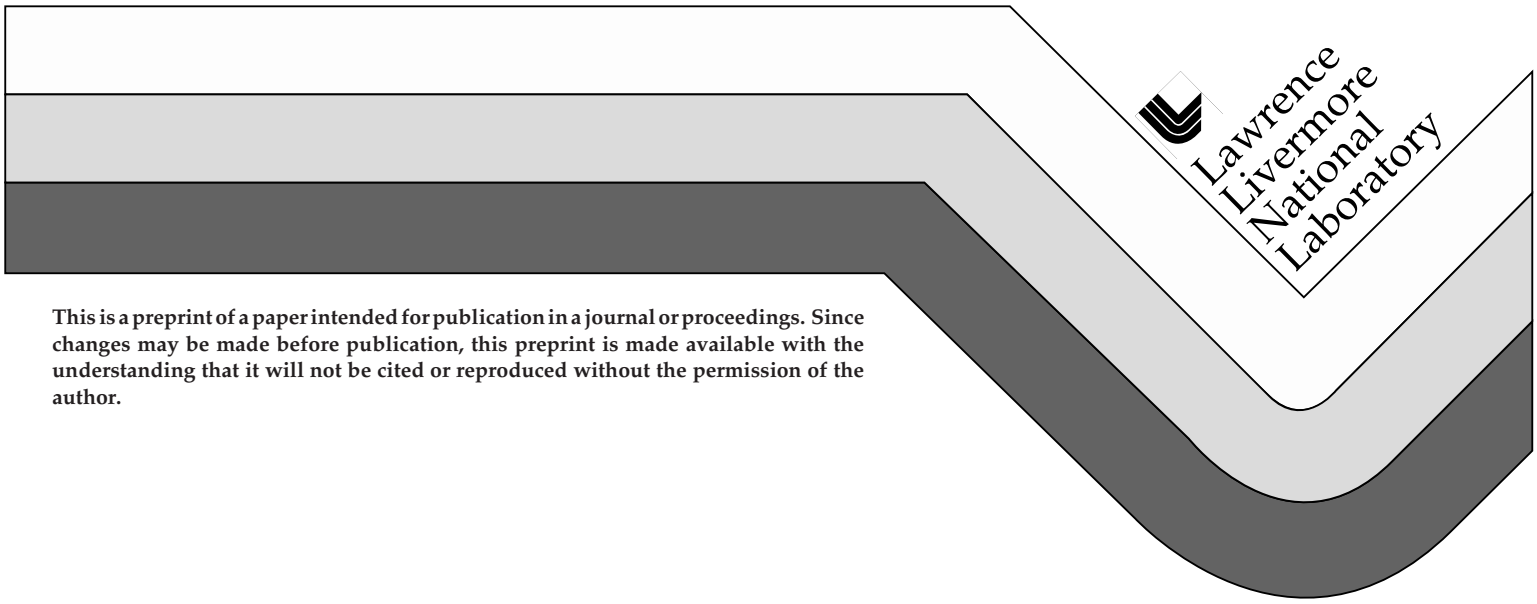

SHIPPING CONTAINER RESPONSE TO THREE SEVERE RAILWAY ACCIDENT SCENARIOS*

Gerald C. Mok
Larry E. Fischer
Susarla S. Murty
Monika C. Witte
Fission Energy and Systems Safety Program
Lawrence Livermore National Laboratory
Livermore, California 94551

ABSTRACT

The probability of damage and the potential resulting hazards are analyzed for a representative rail shipping container for three severe rail accident scenarios. The scenarios are: (1) the rupture of closure bolts and resulting opening of closure lid due to a severe impact, (2) the puncture of container by an impacting rail-car coupler, and (3) the yielding of container due to side impact on a rigid uneven surface. The analysis results indicate that scenario 2 is a physically unreasonable event while the probabilities of a significant loss of containment in scenarios 1 and 3 are extremely small. Before assessing the potential risk for the last two scenarios, the uncertainties in predicting complex phenomena for rare, high-consequence hazards needs to be addressed using a rigorous methodology.

1.0 INTRODUCTION

The Modal Study documented in "Shipping Container Response to Severe Highway and Railway Accident Conditions" (Ref. 1) evaluated the responses of a rail shipping container to 24 train accident scenarios as listed in Figure 1. Concerns have arisen that other accident scenarios should have been explicitly included in the evaluations. Three additional scenarios have been identified as being of particular concern. The three scenarios are: (1) impact resulting in the potential separation of the shipping container cask closure from the main body, (2) puncture of the shipping container wall by a railcar coupler, and (3) impact on an uneven surface such as a rock outcropping.

The three additional scenarios appear to be subsets of the original 24 scenarios. The closure separation scenario is an extremely low-probability event of high-velocity, low-angle impact onto (unyielding) hard rock portrayed in the original scenarios 6, 11, and 14. The coupler puncture scenario is an improbable event where the coupler does not fail in scenario 21. The uneven surface scenario is a subset of scenarios 5, 6, 10, 11, 13, 14, 16 and 17 (flat versus uneven surfaces).

The evaluations of these three additional impact scenarios are presented in Sections 2, 3, and 4 of this paper. In Section 5, the qualitative effect on the probability hazard estimates is discussed.

2.0 RUPTURE OF CLOSURE BOLTS AND COMPLETE SEPARATION OF CLOSURE LID AND BODY

The representative rail cask described in the Modal Study report is analyzed here (Figure 2). The cask is assumed to have 30, 1.5-inch closure bolts (ASME B&PV code spec. SB-637, Grade N07718, 150 ksi yield strength and 185 ksi tensile or ultimate strength at room temperature). The tops of

* Work performed under the auspices of the U.S. Department of Energy by the Lawrence Livermore National Laboratory under Contract W-7405-Eng-48.

the bolt heads are located below the outer surface of the closure lid and thus are protected from direct impacts. The cask contents weight is 52000 lb. and the closure lid weighs approximately 8000 lb. The closure lid has two thicknesses (Figure 3), a central lip section of 7 in., and an outer flange section of 3.5 in. The lip section has an outer radius of 34 in.; the flange section and cask have the same outer radius, 38 in.

There are two critical impact conditions for the closure bolts on this typical rail cask: (1) an end impact on the cask bottom, and (2) an oblique impact on the cask top (where the closure lid is located). Condition 1 can cause a spallation of the closure lid or a separation of the closure lid from the cask body, if the lid traps a sufficient momentum to break all closure bolts. Condition 2 can produce a direct impact on the closure lid by the cask contents and cause the closure bolts to break. The following analyses of the representative cask design, however, show that neither of these conditions is likely to result in a total separation of the closure lid and the cask body. Under condition 1, the closure lid can trap sufficient momentum to yield—but not to break—the bolts, while under condition 2 the closure lid is always pinned to the cask body by the impact force at the impacting edge; the closure lid can only be broken open by a very high g-load from the cask.

During an end impact on the bottom (condition 1), a compressional stress wave is generated at the impact end. The wave travels along the cask axis from the cask bottom towards the cask top where the closure lid and bolts are located. When the compressional wave reaches the top, it is reflected as an equal but opposite (tensile) wave which causes a tensile force in the closure bolts. A conservative estimate of this tensile bolt force is obtained using the following assumptions: (1) the impact is perfect; therefore, the wave is uniform over the cask cross-section, (2) the target is unyielding, and there is no impact limiter, i.e., the cask bottom impacts the target directly, (3) the wave is square, which is propagated and reflected without any dissipation and dispersion, and (4) the wave is elastic and its maximum stress is the yield strength of the cask cylinder material (25000 for 304 stainless steel). Assumptions 1 through 3 are idealistic and most likely not achievable. They are used merely to produce a conservative analysis. Assumption 4 is realistic. A plastic wave is itself dispersive. Therefore, it would be rapidly reduced to an elastic wave. Based on these conservative assumptions, a momentum analysis shows that the impact wave can yield all the bolts but cannot produce sufficient bolt elongation to break the bolts. The maximum resulting bolt strain is 0.21% which is far below the tensile rupture elongation of 10%.

During an oblique impact on the cask top (condition 2), the edge of the closure lid nearest the target hits the target first. Until the cask body rebounds, this edge of the closure lid is fixed to the target. However, under the inertial effect of the cask contents and the closure lid itself, the closure lid can still rotate about this fixed edge and be separated from the cask body as shown in Figure 3. This possible separation is resisted by the closure bolts and by the cask inner wall. The small clearance between the cask inner wall and the lip of the closure lid prevents the lid from rotating freely. Thus, the closure lid cannot be pushed open unless the inertial force of the cask contents and closure lid exceeds the strength of the closure bolts and cask wall. The minimum force required to push open the closure lid is estimated using the following assumptions: (1) the closure lid is rigid, (2) the entire mass of the contents and the closure lid contributes to the inertial force on the closure bolts, (3) the impact acceleration or deceleration of the contents and closure is the same as cask body, (4) there is no friction, and (5) the closure bolt is failed by axial tension over its cross-sectional area, and the cask wall is failed by shear over an area where the rotating closure lid intersects the cask wall (Figure 3 inset). Using a tensile strength of 185 ksi for the closure bolt, and a shear strength of 45 ksi for the cask wall, the following estimates of the minimum g-load required to push the closure lid fully open are obtained for three clearances between the closure lip and the cask wall: 470 g and 334 g for clearances of 0" and 0.15", respectively. The clearance of 0" is reasonable, because upon impact the clearance between the closure lip and the cask wall on the edge opposite the impact edge is expected to vanish due to pushing by the impact force.

The Modal Study analysis results (Reference 1) show that in an endwise impact, the 470 g load level can only be attained for velocities greater than 82 mph and on an unyielding surface. In reality, the impact force is not expected to reach 470 g unless the impact velocity is significantly greater than 82 mph. This is because at this force level (in excess of one million pounds), a real surface including hard rock will not behave like an unyielding surface. A real surface will deform, yield, or fracture and absorb a significant amount of impact energy. Thus, a significantly greater impact energy or velocity will be needed to generate the same impact force as that on an unyielding surface. Nevertheless, for the present study, the conservative velocity limit of 82 mph is used. Using this information and the accident scenarios listed in Figure 1, the probability or likelihood of bolt failure and cap lip shearing leading to the release of contents from the representative cask is estimated to be less than 5×10^{-10} per accident. The hazards of this rare event are similar to the high-consequence hazards shown in Figure 4 for strains above 30%. However, a quantitative estimate of the increased risk due to this rare event with potentially high-consequence hazards is not attempted here, because, as discussed in Section 5.0, such an analysis will require a study of the uncertainties in predicting the complex cask-closure failure phenomenon.

3.0 COUPLER PUNCTURE

The following analysis shows that the 2.5" outer cylindrical wall of the representative rail cask cannot be punctured by a regulatory puncture bar or by a typical rail-car coupler. Both the puncture bar and the coupler are

expected to yield or fail before the puncture force can be fully developed in the cask wall.

The minimum force required for puncturing is estimated here using an empirical method developed by Larder and Arthur (on 316 stainless steels). Their study shows that a puncture occurs when the shear stress in the cask outer wall along the puncture bar circumference attains the shear strength over the entire thickness of the cask wall. The shear strength is 60% of the tensile strength of the cask wall material. Thus, the minimum puncture force is the product of the shear strength, the puncture bar circumference, and the cask outer wall thickness. This force is 2.12 million pounds, if the regulatory puncture bar is used. The same force should be near 8.1 million pounds, if a typical rail coupler is used as shown in Figure 5. This estimate assumes that a typical coupler has an 18" square punch cross-section. A typical coupler has an uneven front surface containing several spike-like short protrusions of 3" to 4". The spikes may be able to produce local indentation to the cask outer wall, but the total puncture of the cask wall can only be accomplished by the large square base of the coupler. The required puncture force of 8.1 million pounds for the rail cask is significantly greater than the puncture force required for a rail tank car whose typical thickness varies from 7/16" to 13/16". Using the same rail coupler, the puncture force for a rail tank car of these thicknesses can be shown to vary from 1.1 to 2.0 million pounds, which is less than one-fourth of the required force for the rail cask. Thus puncturing of a rail cask is significantly more difficult than puncturing a rail tank car.

It is very doubtful that the regulatory puncture bar and the rail coupler can produce the foregoing estimated puncture forces for the typical rail cask. In the case of the coupler, the draft gear or shock absorber behind the coupler will yield before the large required puncture force of 8.1 million pounds can develop. Typically, a draft gear is designed to limit the collision force to less than 100 tons to minimize possible damages during coupling operations. Similarly, the regulatory puncture bar can be shown here to yield and buckle before the puncture force of 2.12 million pounds can be fully developed. This conclusion concerning the puncture bar is from an analysis using the following assumptions: (1) the regulatory puncture bar is a solid circular cylinder of 6" in diameter and made of mild steel (a regulatory requirement), (2) the mild steel has a yield stress and proportional limit of 36 ksi and an ultimate stress of 58 ksi (ASTM A36 structural steel), (3) the puncture bar is totally fixed at its base and is free to translate but not to rotate at its puncture end, and (4) the puncture bar has a length of 8", which is the minimum required for puncturing through the 8" cask wall thickness which consists of a 2.5" 304-stainless-steel outer wall plus a 4" lead shield plus an 1.5" 304-stainless-steel inner wall. (The estimated puncture force of 2.12 million pounds is only for the 2.5" outer shell. The force required for puncturing through the three layers of the cask wall should be greater. Therefore, the force estimate is conservative for the present analysis.) Using the foregoing assumptions, the puncture bar can be shown to yield and buckle under an axial compressive load of 1.02 million pounds. The puncture bar buckles plastically; therefore, the buckling load is significantly lower than the elastic buckling load of 7.18 million pounds.

The foregoing conclusion on the impossibility of puncturing the cask wall is conservative, because it omits additional existing resistance to puncturing. In the case of the rail coupler, the structure of a rail car or locomotive may also help prevent puncturing, because a coupler usually protrudes only a few inches in front of a rail car or locomotive. As soon as the coupler draft gear yields, the body of the rail car or locomotive will touch the cask to reduce the puncture load at the coupler. In addition, the required puncture load of 8.1 million pounds is significantly higher than the structural load-carrying capacity of a rail car and possibly of a locomotive. Using nonlinear finite element analyses, Eggers estimated that the axial load carrying capacity at the coupler location is about 0.90, 3.6, and 4.64 million pounds for the base frame structure of a 40-50-ton standard rail box car, a 150-ton rail freight car, and a typical diesel locomotive, respectively. Therefore, it is very likely that the impacting rail cars and locomotive would not be able to support the required 8.1-million-pound puncture load even if the coupler did not yield. (The same conclusion, however, cannot be made for a rail tank car, whose puncture force varies from 1.1 to 2.0 million pounds as estimated earlier. A locomotive or a rail freight car can produce the required puncture force for a tank car if the coupler does not yield.) In the case of the regulatory puncture bar, the evaluation in the preceding paragraph ignores the inevitable deflection of the cask wall under the puncture load. The cask wall deflection will add to the minimum length requirement of the puncture bar and limit the growth of the puncture force. The expected cask wall deflection under the puncture load can be estimated using the static sidewise force-deflection curve of the rail cask (Figure E-21 of the Modal Study report). Since the static sidewise loading on the cask is similar to applying two identical puncture loads on opposite sides of the cask, the cask deflection given in the figure is used as two times the deflection generated by a puncture force. Thus, the deflection at the puncture load of 2.1 million pounds is approximately 10". If this deflection allowance is added to the puncture bar length, the puncture bar will certainly buckle before puncturing. If it is not added, the cask body will touch the rigid support of the puncture bar and the puncture load will be significantly reduced.

Once the puncture bar or the rail coupler yields, the impact condition and resulting damage should not be very different from those of a cask impacting an unyielding target, a rail car, or a locomotive.

4.0 UNEVEN SURFACE

Analyses were performed for the representative rail cask impacting (at various velocities) a 2-ft.-wide, 1-ft.-high, and

100-in.-long concrete bump. The DYNA3D computer program was used with the finite element model depicted in Figure 6. Taking advantage of the geometric symmetry of the problem, only one half of the rail cask and concrete bump was modeled. Following the same conservative approach of the Modal Study, only the mass—and not the stiffness of the cask contents—was represented in the analysis model, so that the cask strain obtained will be greater than the actual value. The contents mass was evenly distributed to the two end caps of the cask. The lumping of the mass to the end cap provides additional conservatism to the maximum strain results. Figure 7 presents the peak rigid-body deceleration (g-load) and the maximum effective strain of the inner shell of the cask obtained for various impact velocities.

Comparing the present results to the analysis results reported in the Modal Study report for side drops of the rail cask onto a flat rigid surface, the present g-loads are significantly higher for the same impact velocity. The higher g-load is mainly due to the stiffness of the end caps which was included in the present analysis but not in the previous side drop analysis. However, the results of these two sets of analyses are not significantly different in the maximum inner-shell strain. This similarity in the strain result indicates that the inner-shell strain is determined mainly by the stiffness of the cask body rather than by the stiffness of the end caps and the target.

The primary difference between impacting on a flat surface versus an uneven one is that impact limiters do not provide protection for low-velocity impacts which are more probable than high-velocity impacts. In order to bypass the impact limiter, the outcropping or uneven surface should protrude at least 25 inches to get the full effect. Also, the impact angle should be horizontal or nearly horizontal. The likelihood of having large enough protrusions and a nearly horizontal impact is estimated to be .01. The overall likelihood for this type of event for scenarios 5, 6, 10, 11, 13, 14, 16, and 17 is approximately 3×10^{-5}. The probability will be further reduced depending on the impact velocity and damage to the cask. Qualitative estimates predict that higher hazards could occur at lower velocities for uneven versus flat surfaces with some increase in risk. To quantitatively estimate the increased risk, the uncertainties in predicting complex phenomena for rare, high-consequence hazards must be addressed as suggested in Section 5.0.

5.0 CONCLUSIONS AND RECOMMENDATIONS

Scenarios which result in very low to rare probabilities with potentially high consequence hazards should have an uncertainty analysis performed on them. The closure lid failure and uneven surface scenarios are good examples where uncertainty analyses should be performed.

One approach to address uncertainty is to develop uniform guidance which has been agreed upon by a prestigious committee. Guidance has been developed by the Senior Seismic Hazard Analysis Committee (SSHAC) for performing Probabilistic Seismic Hazard Analysis (PSHA) (Ref. 2). The guidance includes methods for proper and full inclusion of uncertainties and inclusion of the range of diverse technical interpretations supported by available data.

Alternatively, Professor Theofanous of University of California, Santa Barbara (UCSB), has developed an alternate approach called the Risk Oriented Accident Analysis Methodology (ROAAM) to assess and manage extremely severe nuclear reactor accidents (Ref. 3). The methodology uses risk assessment to identify rare, high-consequence hazards and their uncertainties. Experiments are then conducted to demonstrate that by using defense-in-depth techniques, the high consequence can be sufficiently mitigated to be physically unreasonable and thus address the uncertainties. Either or both of these approaches might be used to assess and manage the risk in spent fuel transportation and to bring better closure with the public.

6.0 REFERENCES

1. Fischer, L. E., C. K. Chou, M. A. Gerhard, C. Y. Kimura, R. W. Martin, R. W Mensing, M. E. Mount, and M. C. Witte. “Shipping Container Response to Severe Highway and Railway Accident Conditions.” Volume I: Main Report, NUREG/CR-4829 (UCID-20733), Vol. 1.

2. Budnitz, R.J., G. Apostolakis, D. M. Boore, L. S. Cluff, K. J. Coppersmith, C. A. Cornell, P. A. Morris. “Recommendations for Probabilistic Seismic Hazard Analysis: Guidance on Uncertainty and Use of Experts.” Prepared by the Senior Seismic Hazard Analysis Committee (SSHAC) for the Nuclear Regulatory Commission (NRC), NUREG/CR-6372 (UCRL-ID-122160), April 1997.

3. Theofanous, T.G. “On the Proper Formulation of Safety Goals and Assessment of Safety Margins for Rare and High-Consequence Hazards,” Spring 1996. Invited for a special issue on “Aleatory & Systemic Uncertainty in Performance Assessment of Complex Systems” in *Reliability Engineering & Systems Safety*, in press.

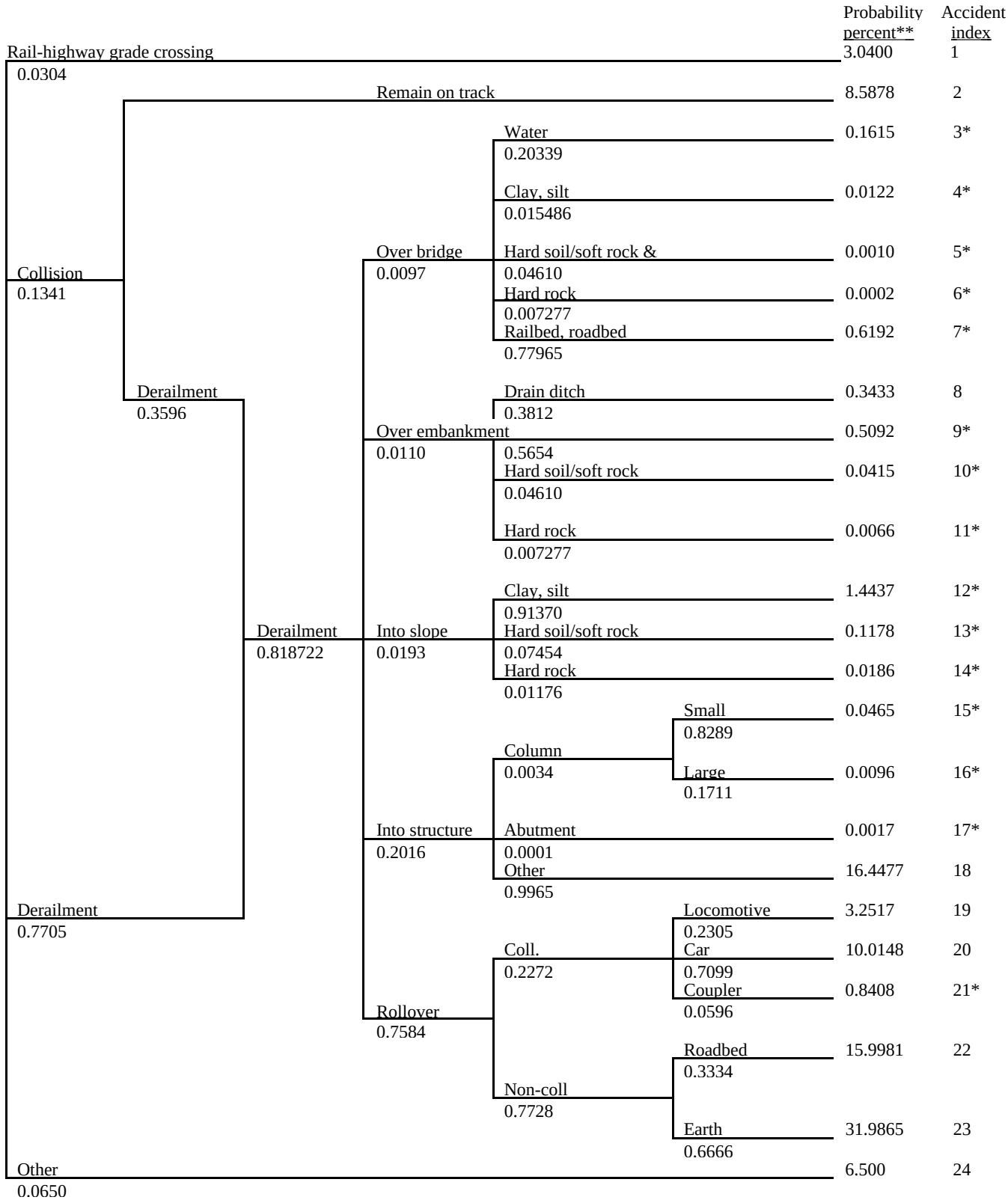

*Potentially significant accident scenarios

**Conditional probability which assumes an accident occurs

FIGURE 1. RESPONSES OF A RAIL SHIPPING CONTAINER TO 24 TRAIN ACCIDENT SCENARIOS

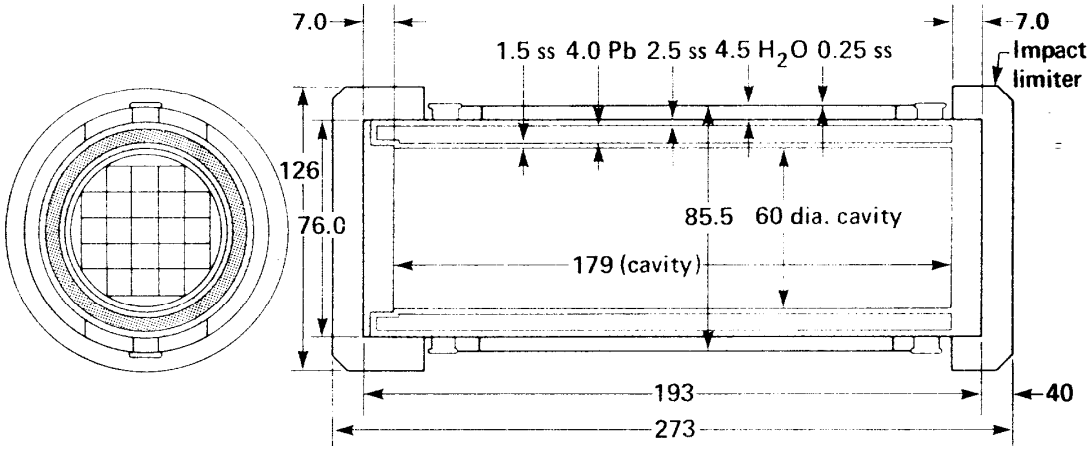

All dimensions in inches

Item	Weight, lbs
Body	122,500
Limiter	22,500
Contents	52,000
	197,000

FIGURE 2. REPRESENTATIVE RAIL CASK DESIGN USED FOR DYNAMIC STRUCTURAL AND THERMAL RESPONSE STUDIES

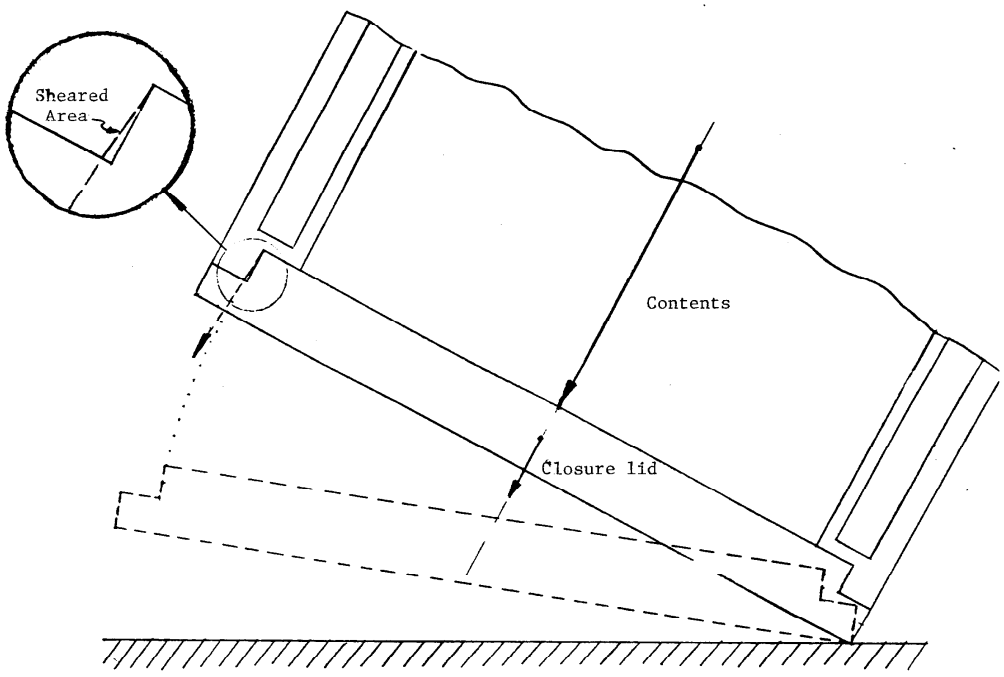

FIGURE 3. CLOSURE IMPACT OF REPRESENTATIVE RAIL CASK ON UNYIELDING SURFACE

S_3 (30)	(G)4.10E+4 (V)2.96E+3 (P)1.51E+0 (E)1.11E+3	4.10E+4 2.96+3 1.51E+0 1.11E+3	4.10E+4 2.96E+3 1.51E+0 1.11E+0	4.10E+4 2.96E+3 1.51E+0 1.11E+0	4.10E+4 2.96E+3 1.51E+0 1.11E+3
S_2 (2)	(G)2.14E+4 (v)2.96E+2 (P)1.51E-1 (E)1.10E+2	2.14E+4 2.96E+2 1.51E-1 1.10E+2	2.14E+4 2.96E+2 1.15E-1 1.11E+2	2.52E+4 2.96E+2 1.15E-1 1.11E+2	4.10E+4 2.96E+3 1.51E+0 1.11E+3
S_1 (0.2)	(G)2.14E+3 (V)2.96E+1 (P)1.51E-2 (E)2.75E+1	2.14E+3 2.96E+1 1.51E-2 2.75E+1	2.14E+3 2.96E+1 1.51E-2 2.85E+1	2.14E+3 2.96E+1 1.51E-2 2.85E+1	4.10E+4 2.96E+3 1.51E+0 1.11E+3
	(G)~0 (V)~0 (P)~0 (E)~0	6.40E+2 8.88E+0 4.56E-3 ~0	6.40E+2 8.88E+0 4.56E-3 1.00E+0	2.52E+4 2.96E+2 1.51E-1 1.00+0	4.10E+4 2.96E+3 1.51E+0 1.11E+3
	T_1 (500)	T_2 (600)	T_3 (650)	T_4 (1050)	

Thermal Response (lead mid-thickness temperature, °F)

(G)=Noble gases, curies | **(P)=Particles, curies** | **E+x=10^x**
(v)=Vapors, curies | **(E)=Exposure, curies**

FIGURE 4. RADIOLOGICAL HAZARDS ESTIMATED FOR RESPONSE REGIONS FOR REPRESENTATIVE RAIL CASK

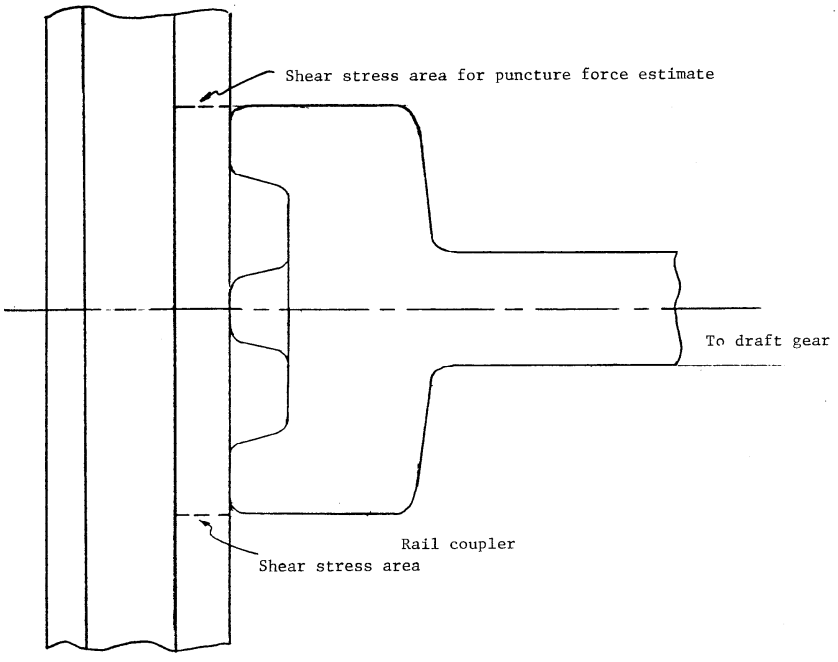

FIGURE 5. COUPLER IMPACT ON REPRESENTATIVE RAIL CASK WALL

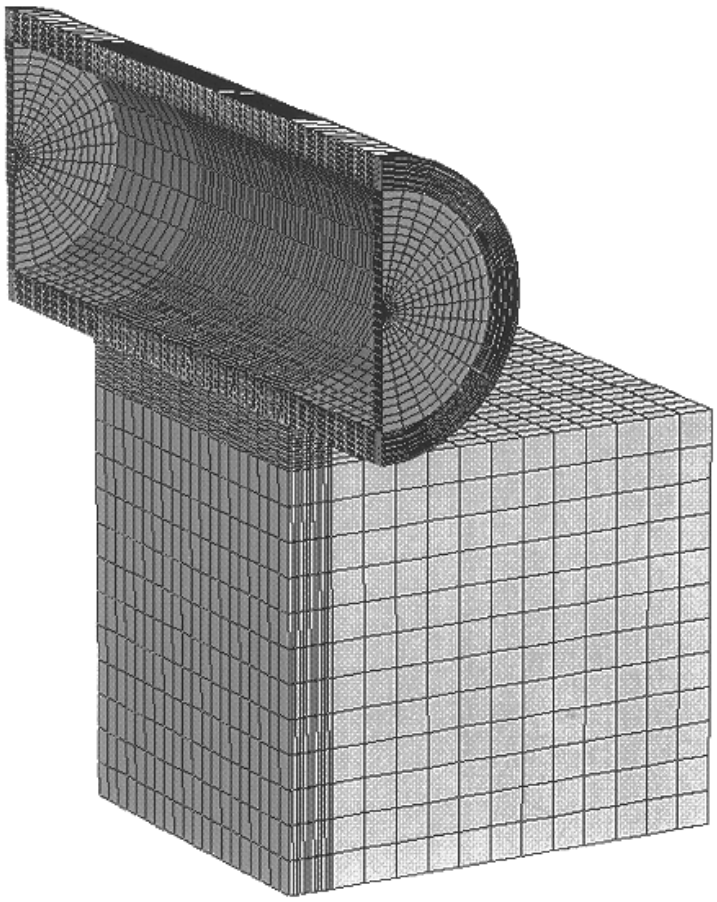

FIGURE 6. RAIL CASK SIDE DROP ON UNEVEN SURFACE

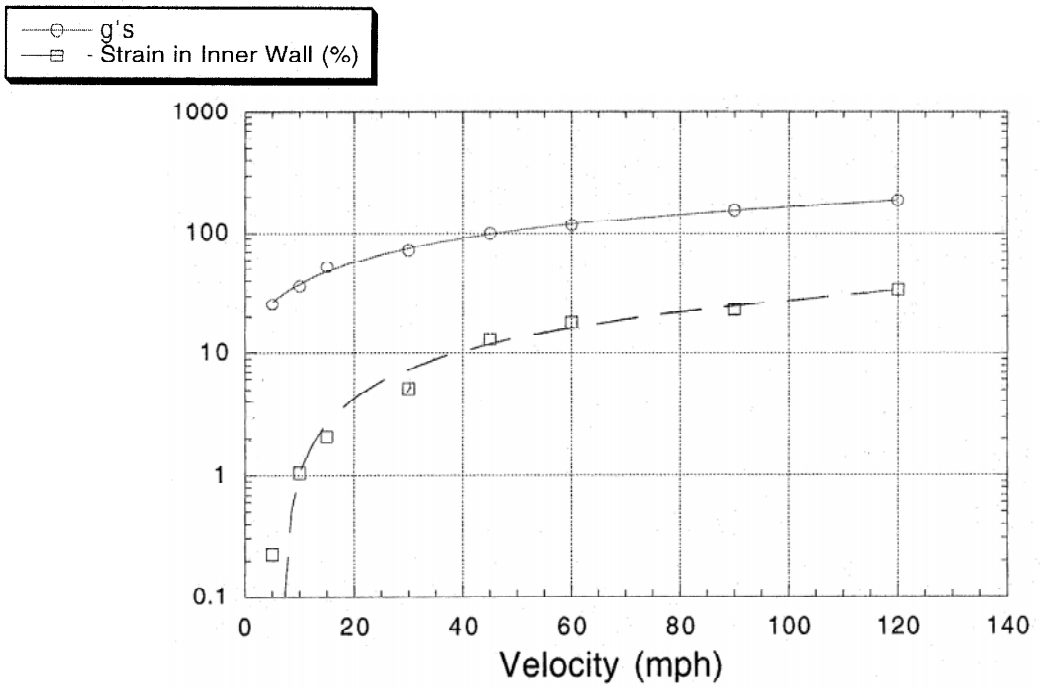

FIGURE 7. RAIL CASK IMPACTING 2 FT. X 100 IN. CONCRETE BUMP WITHOUT LIMITERS (CUBIC CURVE FIT)

Technical Information Department • **Lawrence Livermore National Laboratory**
University of California • Livermore, California 94551